Energy and momentum resolved band structure of K_2O : electron momentum spectroscopy and linear combination of atomic orbitals calculation

2003 J. Phys.: Condens. Matter 15 6955

(http://iopscience.iop.org/0953-8984/15/41/005)

INSTITUTE OF PHYSICS PUBLISHING JOURNAL OF PHYSICS: CONDENSED MATTER

J. Phys.: Condens. Matter **15** (2003) 6955–6968 PII: S0953-8984(03)67395-9

Energy and momentum resolved band structure of K_2O: electron momentum spectroscopy and linear combination of atomic orbitals calculation

E A Mikajlo[1] **and M J Ford**[2]

[1] School of Chemistry, Physics and Earth Science, Flinders University, GPO Box 2100, SA 5001, Australia
[2] Institute for Nanoscale Technology, University of Technology, Sydney, PO Box 123, Broadway NSW 2007, Australia

E-mail: mike.ford@uts.edu.au

Received 7 August 2003
Published 3 October 2003
Online at stacks.iop.org/JPhysCM/15/6955

Abstract

This paper details an experimental and theoretical investigation into the electronic structure of the highly ionic, alkali oxide, potassium oxide (K_2O). The experiments were carried out using the relatively new technique of electron momentum spectroscopy. This is an electron impact technique that is capable of measuring the electron intensity distribution as a function of energy *and* momentum. Calculations were performed within the linear combination of atomic orbitals approximation using both Hartree–Fock and density functional theory formalisms. We have been able to map the band dispersions and intensities in the oxygen valence bands and potassium 3p and 3s bands for the first time. Overlap of the O 2s and K 3p binding energy peaks makes it difficult to extract the band gaps involving either of these bands. The O 2p and K 3s peaks are resolved, however, and we observe a gap of 30.4 ± 0.2 eV. This value is reproduced by the PBE0 calculation. Intensities within the s bands are reproduced well by all our calculations, whereas the observed p bands show anomalous intensity at the Γ-point, which is not present in any of the calculations.

1. Introduction

Our understanding of the solid state has progressed to the stage where for simple, relatively small condensed matter systems *ab initio* calculations are relatively routine. In the case of metallic and semiconducting materials results of these calculations are usually compared with the available experimental results; typically photoemission measurements of the densities of states, optical and x-ray measurements of transitions between special points within the band structure, and Compton profiles of the momentum distribution. Angle resolved photoemission

spectroscopy measurements (ARPES), where the complete band dispersion is mapped in both energy and momentum, can provide a sensitive test of band structure calculations. ARPES data exist for a number of metallic and semiconducting solids.

Ab initio methods have proven to be successful in the case of metals and semiconductors. Their universal application, however, remains untested due to the lack of experimental electronic structure data for ionic solids. The motivation for the present work is to bridge this gap and provide an experimental mapping of the band structure of a prototypical ionic solid, K_2O. Our technique of electron momentum spectroscopy (EMS) provides both the band dispersion, as with ARPES, together with the band intensities, and can be applied to ionic materials with crystalline, polycrystalline or amorphous structures. We compare these experimental results with calculations based upon the linear combination of atomic orbitals (LCAO) approximation. The aim of the comparison is to assess the relative merits of the Hartree–Fock (HF) method versus representative density functional theory (DFT) methods for predicting electronic structures. While the application of these methods to predicting structural properties such as lattice and elastic constants has been relatively well explored for some ionic systems, electronic properties are not so well represented in the literature. This paper also represents an extension of our previous work on the lighter group I and group II oxides [1, 2].

From a computational point of view, K_2O is a relatively simple system to model. Like the lighter alkali oxides it crystallizes into the anti-fluorite structure. With 46 electrons in the unit cell, only relatively small computational resources are required for high quality calculations. Despite this, K_2O has been the subject of very few computational studies. Dovesi *et al* [3] completed an *ab initio* study for the three lightest alkali oxides. In their work the variational basis sets for K_2O were optimized and the calculated total binding energy, equilibrium lattice parameter, elastic constants and central zone phonon frequencies reported. Zhuravlev *et al* [4] have published DFT, plane wave calculations for the band structure and densities of states of a number of alkali metal oxides and sulphides including K_2O. Their study focuses primarily on the valence and unoccupied bands and does not compare or test their results with experimental data.

From an experimental point of view K_2O is not so simple: it readily forms a number of oxide species and its highly insulating nature makes it problematic in photoemission measurements. Potassium hyperoxide, oxide, peroxide and superoxide species have all been identified and reported in the literature [5]. This chemical diversity has attracted much attention and many research groups have made attempts to understand the chemistry of the complex potassium–oxygen interactions. The majority of these studies started with single crystals or polycrystalline films of potassium and by increasing the oxygen pressure at a variety of temperatures have been able to generate the different potassium–oxygen species. Photoemission spectroscopy has typically been used to identify each of the species present. Whilst a number of photoemission reports for the K_2O electronic structure of core and valence states are found in the literature [6–9], to our knowledge no results for the complete electronic structure, resolved in both energy and momentum, exist. This lack of detailed results prevents thorough testing of theoretical methods.

More recent experimental investigations have focused on the absorption of oxygen on potassium covered transition metal surfaces [10, 11]. This area of research has attracted significant interest due to its relevance to heterogeneous catalysis. The catalytic properties of K promoters are well known and are believed to be present on the surface of working catalysts as alkali metal compounds such as potassium oxide. While some of this work reports the electronic structure of K_2O using x-ray photoemission spectroscopy (XPS) and ultraviolet photoemission spectroscopy (UPS), still no momentum resolved data exist.

We compare the results from our EMS experiments with tight binding calculations performed using the commercial CRYSTAL98 software package [12] at both the HF and DFT levels. The experimental and theoretical results presented here build on existing studies by providing energy *and* momentum resolved experimental electron intensities and comparing these with four different theoretical schemes. This work reveals aspects of the theoretical models that are not apparent from previous structural studies alone [3].

2. Experiment

EMS is now an established technique [13] with a number of publications detailing the experimental design of the (e, 2e) spectrometer used in this work [14, 15]. In brief, EMS ionizes the target through medium energy (20 kV) electron impact and subsequently measures the energy and momenta of the two outgoing electrons. Using conservation laws it is then possible to obtain a ground state electron density map resolved in both energy and momentum. In this technique the real momentum of the electrons, rather than crystal momentum, is measured and thus the technique is equally suited to crystalline, polycrystalline and amorphous materials.

The experiment operates in transmission mode and therefore the targets to be investigated must be made as thin as is practicable (in practice around 10 nm) to minimize multiple electron scattering. This requirement is the major limitation on the general application of EMS. The relative surface sensitivity of the technique, however, means that ionic samples can be prepared by evaporation using a 3 nm thick am-C film as a support. The measured EMS signal comes predominantly from the outermost 2 nm of the target; the remaining thickness produces a background signal. This depth sensitivity is associated with the path length of one of the outgoing electrons detected at the relatively low energy of 1.2 keV.

In this paper potassium of 99.95% purity was thermally evaporated in an oxygen background of 1×10^{-6} Torr. The typical background pressure in the evaporation chamber was of the order of 1×10^{-10} Torr. An evaporation rate of 0.2 Å s^{-1} as measured on a quartz crystal microbalance was used, corresponding to an O/K impinging ratio of approximately 0.2. In the work by Jupille *et al* [7] various potassium–oxygen species were prepared through a direct evaporation of potassium in an oxygen environment. For each of the potassium oxide species identified, they provide an oxygen/potassium (O/K) impinging ratio that led to the production of that particular oxide. For the least oxygen rich species, K_2O, their preparation was conducted at 100 K at a pressure of 1.5×10^{-7} Torr with an O/K impinging ratio of 0.5. A large increase in the O/K impinging ratio to 18 was required to produce a dominant K_2O_2 species. It is therefore reasonable to expect that K_2O rather than the peroxide is produced in our case.

K_2O films of various thicknesses were prepared to determine the optimum coverage ensuring that the underlying amorphous carbon did not contaminate the results while minimizing the effects of multiple scattering. A 2.4 nm overlayer of K_2O on the am-C substrate provided the best compromise. Figure 1 shows the Auger spectra of this sample immediately prior to and after evaporation of the potassium together with that after three days of constant EMS measurement. Using standard sensitivity factors [16] the post-evaporation spectrum (b) suggests a potassium to oxygen ratio of 4:1. Determining stoichiometries from Auger data is problematic and certainly our value does not correspond to any of the possible oxide species. It could also suggest the presence of unoxidized potassium. Our EMS measurements, however, would be sensitive to this and there is no indication of a free-electron-like parabola from the metal in our band structure measurement. The least oxygen rich species, K_2O, has the stoichiometry closest to our value. A small carbon KLL transition is apparent in (b) and after three days in the spectrometer (c) the intensity of this transition increases by a factor of

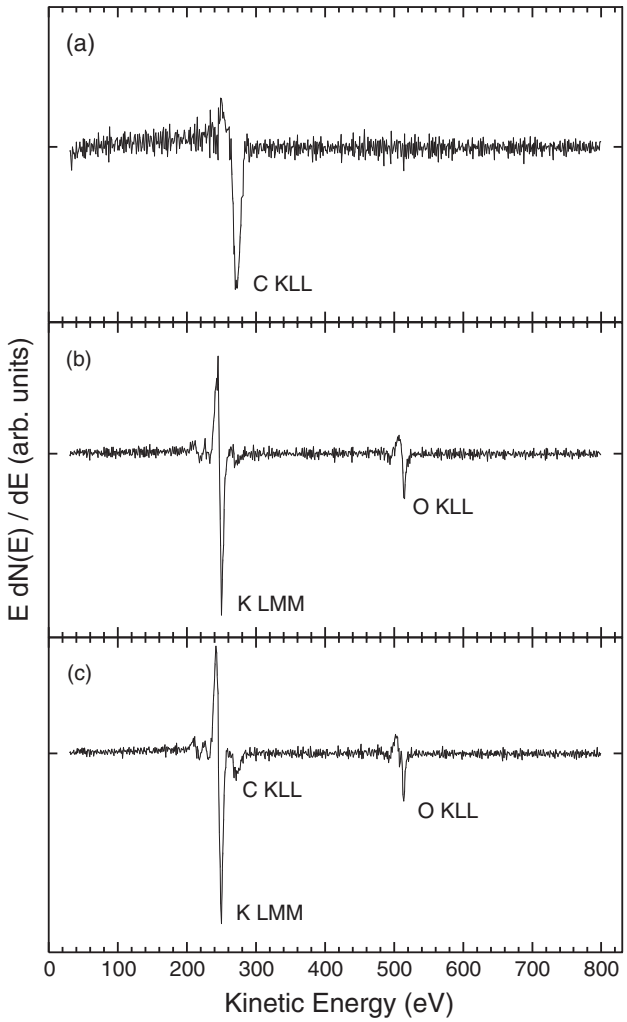

Figure 1. Auger spectra of (a) the amorphous carbon substrate, (b) the potassium oxide overlayer immediately after evaporation and (c) after 72 h of electron irradiation in the spectrometer.

two. To minimize the effects of this increase in the carbon signal in the (e, 2e) results, two identical samples were prepared and measured for approximately three days each. In this way, a minimal contribution of the am-C substrate appears in the final EMS spectrum.

The (e, 2e) spectrometer used in this work is able to collect data over a 70 eV energy window. This allows for measurement of both the valence and semi-core levels of the group I oxides in a single experiment so accurate determination of band gaps is possible. The overall energy and momentum resolution of the spectrometer are approximately 1 eV and 0.1 au respectively [15]. A small incident beam current of around 90 nA is used. Even though the exposure time is very large, this extremely small beam current yields total electron doses that are still about the same as in a standard Auger measurement [17]. No shift in the peak energies due to sample charging was observed over the course of the measurements.

Figure 2 shows the EMS data for the 2.4 nm samples. These results were obtained from two identically prepared samples, each measured for approximately 75 h in a background pressure

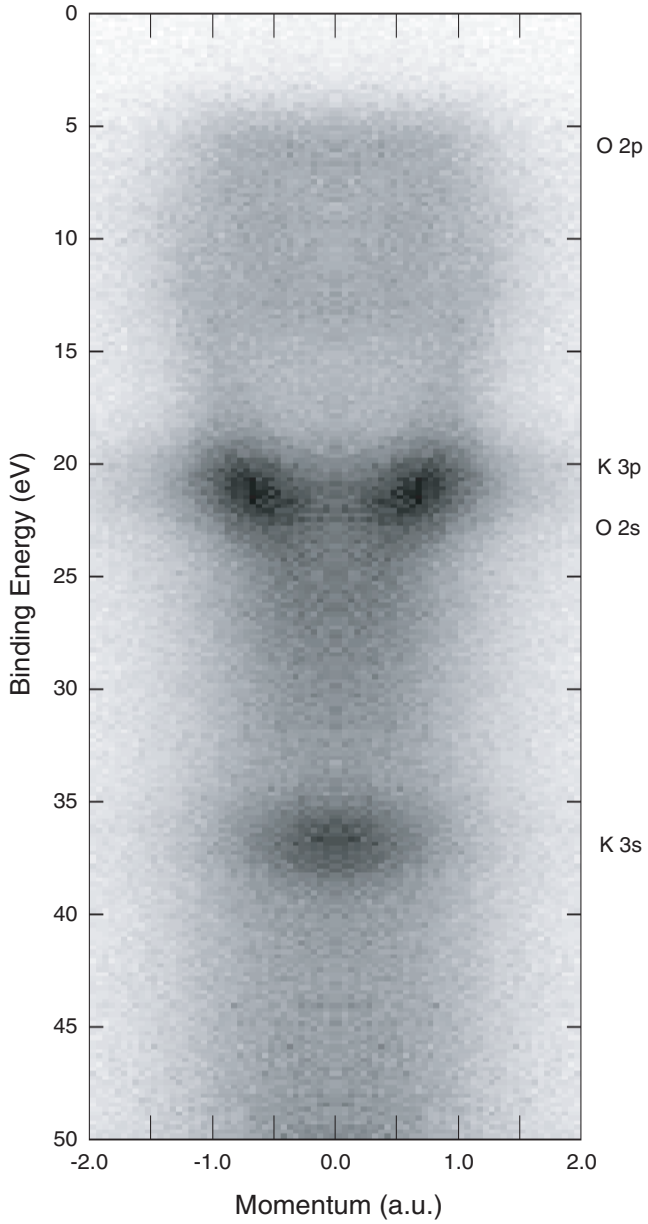

Figure 2. Experimental EMS data for the K_2O sample. Binding energy (eV) is relative to the vacuum level of the spectrometer. Momentum is plotted in atomic units (au). Electron density is represented using a linear greyscale with darker colours indicating higher occupation.

of 8×10^{-10} Torr. The x-axis corresponds to the real momenta of the electrons within the target and is symmetric about zero momentum. This point of zero momentum in the extended zone scheme is equivalent to the Γ-point in typical band structures where crystal momentum is plotted. The y-axis binding energy of the electrons is relative to the vacuum level of the spectrometer which comprises the work function of the sample, any contact potentials present

in either the electron gun or analysers and in principle any charging effects that may occur within the target. The unknown extent of these quantities makes it impossible to comment on the absolute band energies, and for this reason only relative energies are compared with other experiments or calculated results. The z-axis gives a greyscale representation of electron density, with darker colours indicating regions of higher electron occupation. The bands have been labelled according to their predominant atomic orbital character. There is considerable overlap between the O 2s and K 3p bands which are difficult to resolve in the current experiment. We will discuss these points more fully below.

Some additional intensity is present away from the bands in figure 2. The majority of this intensity results from both elastic and inelastic multiple scattering of the (e, 2e) electrons within the target. No band shadows resulting from plasmon excitations are observed in this spectrum indicating that collective plasmon oscillations do not significantly contribute to this background intensity. Whilst the background intensity is more prominent in K_2O than the lighter alkali oxides [2], multiple scattering has still contributed much less to the background in this spectrum than has previously been observed in measurements of metallic [17] and semiconducting materials [18]. This spectrum does not display the characteristic free electron parabola of metallic potassium, suggesting complete oxidation of the sample.

3. Calculations

The CRYSTAL98 [12] package was used to generate the theoretical electronic structures presented in this paper. It has successfully been used by a number of research groups to calculate the structure and a variety of ground state properties for a large range of materials. This package performs *ab initio* calculations to obtain the electronic wavefunction and associated properties for periodic systems in the ground state. To do this it expands the single particle wavefunctions as a linear combination of Bloch functions. These Bloch functions are defined as a linear combination of atomic type orbitals (LCAO), which are in turn defined as a linear combination of Gaussian type functions.

The electronic structure of K_2O was calculated using HF and three DFT Hamiltonians. The functionals employed were Dirac–Slater exchange [19] with Vosko–Wilk–Nusair correlation [20] to represent the local density approximation (LDA), Perdew–Burke–Ernzerhof exchange and correlation [21] for the generalized gradient approximation (PBE) and PBE exchange and correlation mixed with 25% exact HF exchange [22] for the hybrid functional (PBE0).

Due to the relatively small electron count of both potassium and oxygen high quality all electron basis sets recommended by the authors of CRYSTAL98 [3, 12] were used. An 8-411G contraction on the oxygen ion [3, 23] and an 86-511G contraction on the potassium were used [3, 23]. Dovesi *et al* [3] have shown that these relatively small basis sets give reliable results for the group I oxides and that the addition of polarization functions or a second valence shell have relatively small effects on the elastic properties and total ground state energies of these alkali oxides. Addition of a d shell to K in K_2O gives a contraction of the lattice parameter of about 1.3% and less than 3% increase in the two elastic constants.

The calculations presented here were performed at the default tolerances for the CRYSTAL98 package and sampled at 28 points within the irreducible wedge of the Brillouin zone. The characteristic anti-fluorite crystal structure for K_2O, with the experimental lattice constant from Wyckoff [24] of 0.6436 nm, was used in all the calculations. As a check of our calculations we have found optimized lattice constants for each of the four Hamiltonians. The results are presented in table 1.

Table 1. Optimized and experimental lattice parameters.

Method	HF	LDA	PBE	PBE0	Experiment [24]
a_0 (nm)	0.6466	0.6168	0.6414	0.6360	0.6436

As expected the HF method overestimates, albeit very slightly, while LDA underestimates. The gradient-corrected method gives the 'best' result. All predications are within 5% of the experiment. The fact that we have used the experimental lattice parameter rather than optimized values will have very little effect upon our predicted electronic structures, falling below the level discernible by our experiment.

The evaporated experimental samples used in this work are assumed to be polycrystalline in nature, with random crystallite orientations. To simulate this in the calculated results the band structures were averaged over 25 evenly spaced crystal directions within the irreducible wedge of the Brillouin zone [25]. To simulate the experimental resolutions the spherically averaged results were convoluted with Gaussian functions of 0.1 au and 1.0 eV FWHM [15]. The resultant energy and momentum resolved densities can then be directly compared with the output of the EMS spectrometer.

In this paper, calculated band energies and electron momentum densities (EMDs) are given both along definite crystal directions and for the spherically averaged calculations. The energy degeneracy at the Γ-point means that the process of spherically averaging does not significantly affect the band gaps at the Γ-point. Bandwidths vary depending on the crystal direction however, and thus spherically averaging decreases the bandwidths. Whilst comparison of band gaps with other published work is therefore straightforward, comparison of bandwidths requires some caution.

4. Results and discussion

The calculated band dispersions and EMDs at the HF level along the high symmetry [100], [110] and [111] directions within the conventional unit cell are shown in figure 3. Whilst the relative band energies and bandwidths vary between the HF and the three DFT calculations, band shapes remain the same. Using this plot and similar results for the DFT functionals the Γ-point band energies (relative to the valence band maximum) and bandwidths are given in table 2. These data are *not* spherically averaged. The bandwidths have been obtained from band extrema along the crystal direction where band dispersion is greatest.

Comparing tables 1 and 2 we note that structural properties are predicted very well by the HF method and DFT; the basis set has (presumably) been carefully optimized by Dovesi *et al* [3] at the HF level. Electronic properties, on the other hand, are strongly dependent upon the Hamiltonian and less sensitive to the basis set [25]. From table 2 we see that the O 2p–O 2s energy difference decreases by around 30% from the HF method to LDA.

For all four calculations, the shapes of the O 2p and 2s bands in K_2O differ significantly from those of the lighter alkali oxides [2]. Li_2O and Na_2O, like the three lightest alkaline earth oxides [1], have the O 2p band maximum at the Γ-point and show maximum band dispersion in the [111] direction. Conversely, K_2O has the band maximum away from the Γ-point and maximum dispersion is observed in the [110] direction. This same O 2p valence band shape has been observed by Zhuravlev *et al* [4] in their calculations. For the O 2s band, Li_2O and Na_2O possess a band minimum at the Γ-point, whereas in K_2O the Γ-point is at maximum of the dispersion curve. Another difference between the lighter alkali oxides and K_2O is that in K_2O the O 2s and K 3p bands are intermixed, whereas for the other oxides this metal–oxygen band separation is much greater. Presumably this change in shape is due to the size of the metal

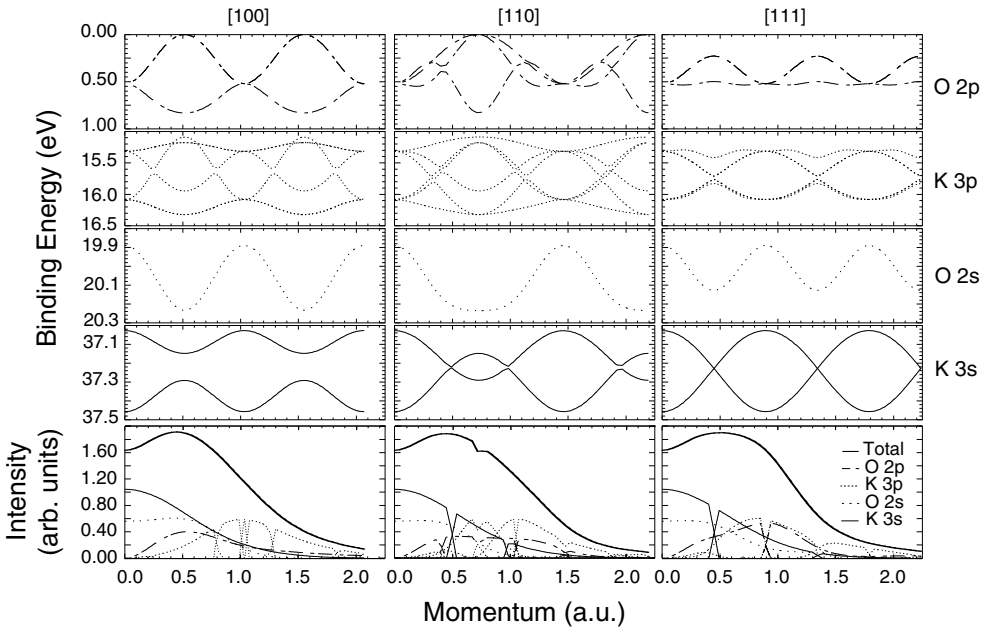

Figure 3. Hartree–Fock (HF) band dispersions and EMDs for K_2O, calculated along three high symmetry directions within the conventional unit cell. Binding energies are relative to the valence band maximum.

Table 2. Γ-point energies, E (eV), relative to the valence band maximum and maximum bandwidths, Δ (eV) (without spherical averaging).

Method	HF	LDA	PBE	PBE0
E O 2p	0.52	0.49	0.47	0.49
E K 3p	15.32	12.67	12.97	13.70
E O 2s	19.89	13.92	14.26	15.72
E K 3s	37.46	29.19	29.68	31.78
Δ O 2p	0.83	0.79	0.75	0.79
Δ O 3p	1.33	1.19	1.12	1.17
Δ O 2s	0.35	0.81	0.75	0.58
Δ O 3s	0.43	0.40	0.37	0.38

ion relative to the oxygen ion and consequently the degree of orbital overlap. We have also carried out some preliminary calculations for Rb_2O and observe the same overall band shapes as in K_2O. Looking at the bandwidths in table 2 we see that the K 3p band is broader than the O 2p band, which is also in contrast to the case for other oxides. This would indicate greater overlap between the 3p orbitals located on the metal ions compared with the p orbitals on the oxygen ions. Again, this is presumably due to the relatively large ionic radius of K compared with Li, Na, or the lighter group II elements. Proximity of the O 2s and K 3p dominated bands may also affect this, giving rise to bands that cannot be so clearly associated with a single atomic orbital.

Figure 4 provides a comparison between the experimental energy and momentum resolved probability density measured by EMS and those calculated with the four theoretical methods. In all four panels the experimental data are identical. The theoretical results are spherically averaged and are prepared by folding the EMD for each band into the band dispersion. For ease

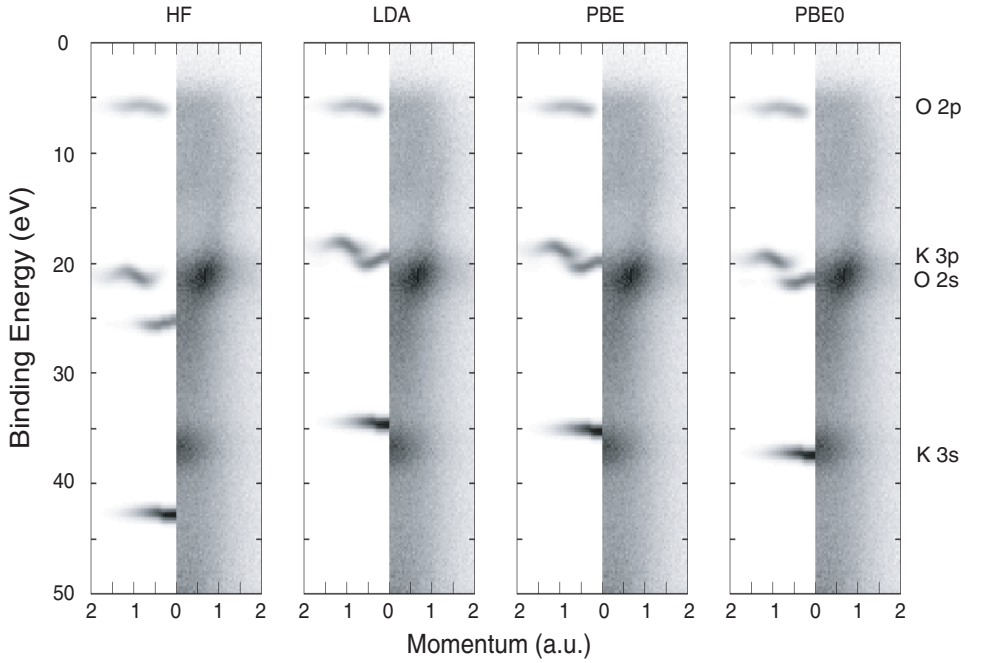

Figure 4. Comparison of experimental and calculated energy and momentum resolved electron densities for K_2O. The experimental data are identical in each panel. Experimental binding energies are relative to the vacuum level of the spectrometer and for ease of comparison the calculated energies have been normalized to the experiment at the Γ-point of the O 2p band.

of comparison, the theoretical data have been shifted to match the experimentally observed binding energy of the O 2p band at the Γ-point. This is necessary because the experimental binding energies are relative to the vacuum level while the calculated ones are relative to the valence band maximum.

The highly ionic nature of K_2O prevents significant overlap of the oxygen valence orbitals with that of potassium and it is therefore appropriate to assign the observed bands to the respective atomic orbitals from which they are derived. Four bands lie within the binding energy range measured; from low to high binding energy these are O 2p, K 3p, O 2s and K 3s. The experimental O 2p band, at approximately 6 eV, has very little intensity and is therefore hard to distinguish from the background. The K 3p and O 2s orbitals overlap in both the experimental and calculated DFT cases. It is not possible to completely resolve the two bands in the experimental data. Finally the K 3s band is easily observed as the band with the highest binding energy in each of the calculations and the experiment.

Qualitatively all four theoretical methods predict a band structure that is similar to the experimental one; however, significant discrepancies exist in relation to relative band intensities, bandwidths and band gaps.

Figure 5 plots the experimental binding energy profiles. Each plot contains the data from figure 4 binned over 0.1 au momentum intervals; the positive and negative momentum components have been summed in order to improve the experimental statistics. Experiment and theory have been normalized in both energy and intensity at the K 3s peak around 37 eV. For clarity not all momentum intervals are shown. In the same figure, to aid comparison with theoretical results, background (fourth order polynomial) subtracted experimental data

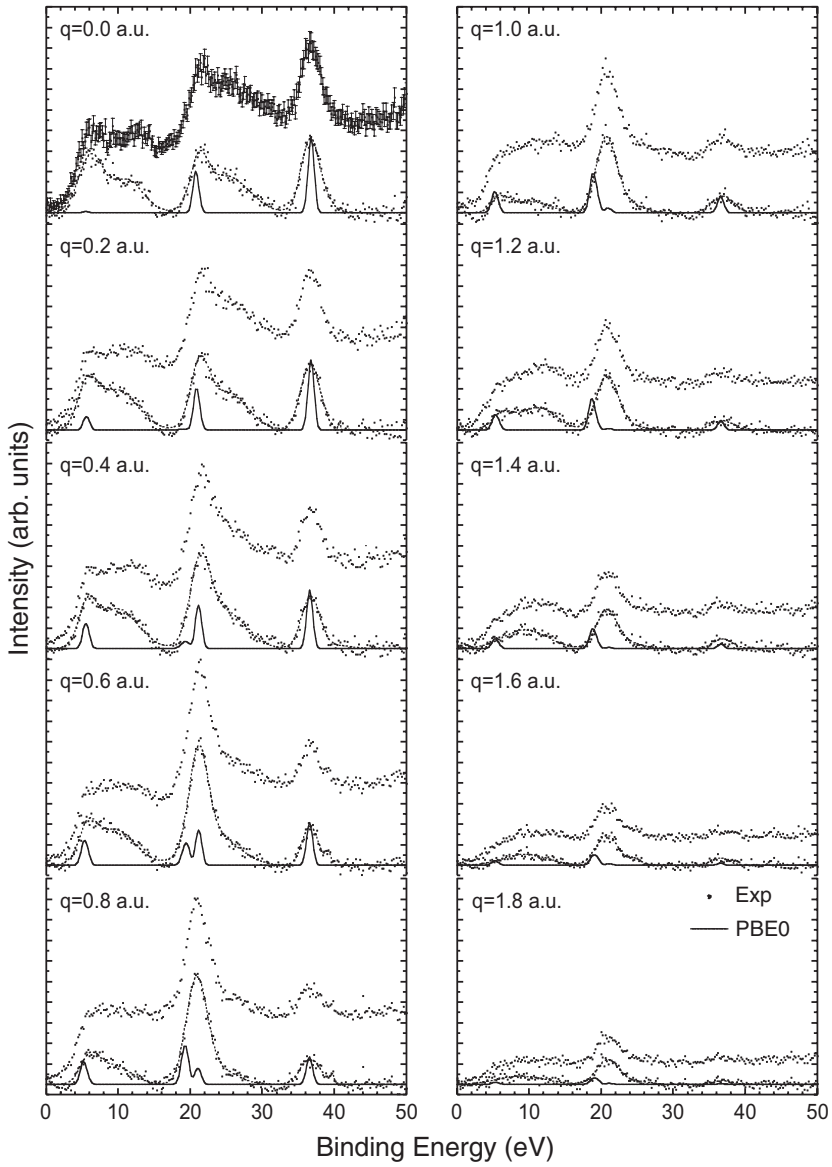

Figure 5. Experimental and DFT hybrid (PBE0) binding energy profiles for K_2O extracted from figure 4 by integrating over 0.1 au momentum intervals. Experimental data are presented with and without subtraction of a smooth background. Binding energies are relative to the vacuum level of the spectrometer and calculated binding energies and intensities have been normalized to the experiment for the K 3s peak in the 0.0 au momentum interval. The experimental error bars presented in the $q = 0.0$ plot are representative for all momentum intervals.

have also been plotted. The theoretical binding energy profiles are those predicted by the hybrid functional, PBE0 (after spherical averaging and convolution to simulate experimental resolutions).

Identification of each of the four contributing bands is simple for the case of the PBE0 prediction in figure 5. From lowest to highest binding energy, they are derived from the

O 2p, K 3s, O 2s and K 3s orbitals respectively. Assigning the experimental peaks in this case is much less precise due to band overlaps, low intensities and background contributions. The experimental O 2p peak occurs at about 6 eV. The next observable peak encompasses both the K 3p and O 2s peaks and is comprised of a well defined peak maximum at 22 eV with a high binding energy shoulder at approximately 25 eV. There is also a shoulder to the O 2p peak at about 12 eV. The DFT calculations predict a splitting between the O 2s and K 3p peaks of 2 eV or less. Hence is it quite possible that the main experimental peak at 22 eV is a convolution of the two bands. The shoulders at 12 and 25 eV could then be due to a small signal from the am-C substrate: the spacing is almost right from the known EMS spectrum of am-C [26], at least at zero momentum. These features, unlike the case for am-C, however, do not seem to disperse in energy at all. An alternative explanation is that the peak at 22 eV and shoulder at 25 eV are the K 3p and O 2s bands respectively. All the calculations predict a lower binding energy for the K 3p peak. In addition, the intensity variation of these two features is consistent with the calculations. Bands derived from s orbitals are expected to have maximum intensity at zero momentum, decreasing monotonically with increasing momentum. Bands derived from p orbitals will have maximum intensity away from zero momentum. Intensity in the shoulder at approximately 25 eV decreases continuously away from zero momentum, losing almost all intensity by 0.8 au. Moreover, the peak at 22 eV appears to reach maximum intensity at around 0.8 au momentum. Finally the K 3s peak is clearly resolved in the experiment at around 37 eV.

Very few published photoemission results reference the O 2s peak. Petersson and Karlsson observe a weak structure at 13.5 eV relative to the Fermi level but also state that the σ_u 2s orbital may be hidden in the complex structure at about 18 eV [8]. In all the valence band spectra published the O 2s band is not clearly visible or even assigned [7, 9, 11]. Previous reports of experimental binding energies for the K 3s peak are consistent with our observations and calculations [8, 9, 11].

The observed band intensities for the O 2p band are dramatically underestimated by the theory at the Γ-point below about 1 au momentum. Above this momentum agreement is reasonable. The K 3s intensity is well reproduced by the calculations. The intensity of the large peak at 22 eV falls well below either the calculated K 3p peak in isolation or a convolution of the K 3p and O 2s peaks. The other theoretical methods employed give very similar intensity distributions to the PBE0 calculation. Spectrometer resolutions and multiple scattering will contribute to the observed intensity at the Γ-point. However, it is unlikely that these mechanisms could redistribute electrons between the measured bands and account for observed differences in peak intensity ratios between the s and p bands. Using a Monte Carlo simulation we have made a preliminary investigation of the contribution of multiple scattering to the anomalous Γ-point intensity [25], and this mechanism does not appear to account entirely for the observed intensity. Spectrometer misalignment may also contribute, although careful calibration of the analyser positions has been undertaken to minimize this source of systematic error. Finally, we cannot rule out the effect of using a relatively thin target or inadequacies in the theoretical models employed.

For a more quantitative analysis of the data in figure 5 and to allow comparison between all our calculations and other work we present Γ-point band gaps and bandwidth data in table 3. Experimental and theoretical binding energy profiles similar to those of figure 5 were fitted with Gaussians, using either one or two Gaussians per peak. This least squares fitting procedure allows us to determine the peak positions, at least for the O 2p and K 3s peaks, reasonably reliably. The experimental and theoretical data were binned into 0.1 and 0.05 au momentum intervals respectively for this purpose. For completeness we have included K 3p, O 2s experimental band gaps assuming that they correspond to the peak and shoulder in figure 5. However, it must be remembered that this interpretation is far from reliable. We do not quote

Table 3. Band gaps measured at the Γ-point and O 2p bandwidth for the experimental data and the spherically averaged theoretical predictions. Units are eV.

	HF	LDA	PBE	PBE0	Experiment
O 2p–O 2s	19.21	13.40	13.80	15.30	18.7
O 2p–K 3s	36.80	28.60	29.20	31.30	30.4 ± 0.2
O 2s–K 3s	17.60	15.20	15.40	16.00	11.7
K 3s–K 3p	22.07	15.8	16.0	18.2	15.3
ΔE O 2p	0.38	0.37	0.30	0.39	0.3 ± 0.2

errors for these band gaps. Our attempts to fit a double Gaussian to the main 22 eV peak also proved extremely unreliable.

The calculated values in table 3 behave as expected. The HF method gives the largest band gaps by quite a long way. All the DFT methods give smaller values, gradient corrections (PBE) increase band gaps slightly over LDA and the inclusion of exact exchange (PBE0) gives a further increase. Bandwidths do not change so noticeably across the four Hamiltonians; these are, remember, spherically averaged bandwidths and in any case dispersion in the O 2p band is very small due to the highly ionic character of K_2O.

Because of the unknown contact potentials in our spectrometer, only energy differences, and not absolute binding energies, can be directly compared between our experiments, *ab initio* calculations and other experimental work. The O 2p–K 3s band gap can be determined more readily from these results because both bands have appreciable intensity at the Γ-point and both are free from band overlap. The experimental value of 30.4 eV is matched best by PBE0, which overestimates this gap by about 3%. The remaining DFT methods underestimate this gap, PBE by 4% and LDA by about 6%. The HF method fares the worst, drastically overestimating this gap by over 21%. This is perhaps the trend one would expect in the calculations but is at odds with our previous observations for the lighter two alkali oxides. There we find that while the DFT methods reproduce oxygen–oxygen band gaps that compare well with HF ones, they do not predict oxygen–metal band gaps very well at all.

For the two lightest alkali oxides PBE0 best predicts the O 2p–O 2s band gap [2]. For K_2O we give a value of 18.7 eV in table 3; surprisingly the best matches is from the HF method, which for the other alkali [2] and alkaline earth oxides [1] grossly overestimates this band gap. PBE0 predicts an intervalence band gap of 15.30 eV, an underestimation of almost 20%. For the metal–metal ion band gap (K 3p–K 3s) the value in table 3 of 15.3 finds best agreement with the LDA calculation. The other methods give values that are too large. Again it must be remembered that these experimental band gaps are difficult to determine due to small intensity and band overlap and that assignment of experimental features is open to discussion.

Bandwidths derived experimentally can also be compared with theoretical predictions. The highly ionic character of K_2O does however prevent significant dispersion in the valence O 2p band. Table 3 shows that all four theories predict O 2p valence bandwidths within 0.09 eV of each other, ranging between 0.30 eV for the PBE method and 0.39 eV for the hybrid method, PBE0. The experimental data have an associated error of approximately 0.2 eV and so cannot be used to distinguish between these calculated values. The remaining bands all have negligible dispersion and we have not, therefore, attempted to extract bandwidths.

5. Conclusions

The electronic structure of K_2O has been successfully measured using EMS, giving the probability distribution of electrons within the target resolved in both energy and momentum

for the O 2p, K 3p, O 2s and K 3s bands. This is the first time the complete band structure, band dispersion and intensity have been measured for this solid. We have also performed electronic structure calculations to compare with our experiment at both the HF and DFT levels. Measurements of this type can provide quantitative tests of theoretical models, an important consideration in the case of ionic solids where the available experimental electronic structure data are relatively sparse.

Assignments of the features in our binding energy spectra are based upon comparison with the calculations. Overall the data show much broader peak structures than for the lighter alkali oxides [2], presumably due to the higher atomic number and hence increased multiple scattering. This, coupled with the small energy separation between O 2s and K 3p, results in our experiment not resolving these two features completely. The O 2p and K 3s bands by contrast are resolved. Apart from in the work of Petersson and Karlsson [8], the location or even presence of the O 2s band has not been reported previously.

From the experimental data it was possible to determine a value of 30.4 ± 0.2 eV for the O 2p–K 3s band gap. Of the DFT methods, PBE0 provides the best predication giving a value within 3% of the experimental one. The HF method grossly overestimates this band gap by more than 21%. The fact that PBE0 predicts the O 2p–K 3s band gap well is perhaps expected, but is in contrast to our observations for the lighter two alkali oxides, where we find DFT performing far better than the HF method for oxygen–oxygen (or metal–metal) band gaps, but the HF method performing better for oxygen–metal band gaps [2]. It must be remembered, however, that strictly speaking DFT does not provide single particle energies, even though such comparisons are often reported and DFT does indeed seem to succeed quite well. Our electronic structure calculations are, to a point, relatively insensitive to the basis set used, but extremely dependent upon the Hamiltonian.

The experimental data display a much higher intensity within the O p bands at the Γ-point than theory predicts. This poor prediction of the intensity within the p bands continues over the entire range of momenta, where there is almost a constant overestimation of the intensity compared with that in the s bands. We observe the anomalous p intensity at the Γ-point in our previous measurements of group I and II oxides. No doubt it is partly due to multiple scattering of the electrons in the target, particularly small angle elastic scattering. Multiple scattering due to plasmon excitation is relatively weak in these oxides. It is unlikely, however, that multiple scattering produces such a large intensity at zero momentum, or can redistribute intensity between the p and s bands. Further, even in Li_2O and BeO where the overall multiple scattering background is small, this intensity effect is equally evident as in the heavier oxides where the overall background is more substantial. Our preliminary simulations of multiple scattering in BeO also indicate that its contribution to the intensity at zero momentum is relatively small. We have taken care to account for systematic instrumental effects due to resolution or spectrometer alignment by careful calibration with carbon samples. These effects contribute, but again they are small. Other systematic effects such as spectrometer sensitivities or sample characteristics may be responsible. In particular, the use of thin targets will give band structures that deviate from those of the bulk. Of course, inadequacies in the theoretical models employed in the calculations cannot be ruled out either.

Acknowledgments

This work was supported by the Flinders University, University of Technology, Sydney, and the ARC. EAM was supported by a SENRAC scholarship. This work would not have been possible without the support of workshop staff at Flinders University.

References

[1] Sashin V A, Dorsett H E, Bolorizadeh M and Ford M J 2000 *J. Chem. Phys.* **113** 8175
[2] Mikajlo E A, Nixon K L, Coleman V A and Ford M J 2002 *J. Phys.: Condens. Matter* **14** 3587
Mikajlo E A, Nixon K L and Ford M J 2003 *J. Phys.: Condens. Matter* **15** 2155
[3] Dovesi R, Roetti C, Freyria-Fava C and Prencipe M 1991 *Chem. Phys.* **156** 11
[4] Zhuravlev Y N, Basalaev Y M and Poplavnoi A S 2001 *Russ. Phys. J.* **44** 398
[5] Vannerberg N-G 1962 *Prog. Inorg. Chem.* **4** 125
[6] Bertel E, Netzer F P, Rosina G and Saalfeld H 1989 *Phys. Rev.* B **39** 6082
Lamontagne B, Semond F and Roy D 1995 *Surf. Sci.* **327** 371
[7] Jupille J, Dolle P and Besancon M 1992 *Surf. Sci.* **260** 271
[8] Petersson L-G and Karlsson S-E 1977 *Phys. Scr.* **16** 425
[9] Qiu S L, Lin C L, Chen J and Strongin M 1990 *Phys. Rev.* B **41** 7467
[10] Broden G, Pirug G and Bonzel H P 1980 *Chem. Phys. Lett.* **73** 506
[11] Hrbek J, Sham T K, Shek M L and Xu G Q 1992 *Langmuir* **8** 2461
[12] Saunders V R, Dovesi R, Roetti C, Causa M, Harrison N M, Orlando R and Zicovich-Wilson C M 1998 *CRYSTAL98 User's Manual* (Torino: University of Torino)
[13] Coplan M A, Moore J H and Doering J P 1994 *Rev. Mod. Phys.* **66** 985
Dennison J R and Ritter A L 1996 *J. Electron Spectrosc. Relat. Phenom.* **77** 99
McCarthy I E and Weigold E 1991 *Rep. Prog. Phys.* **54** 789
[14] Storer P, Caprari R S, Clark S A C, Vos M and Weigold E 1994 *Rev. Sci. Instrum.* **65** 2214
[15] Canney S A, Vos M, Kheifets A S, Clisby N, McCarthy I E and Weigold E 1997 *J. Phys.: Condens. Matter* **9** 1931
[16] Hedberg C L (ed) 1995 *Handbook of Auger Electron Spectroscopy* (Eden Prairie, MN: Physical Electronics, Inc.)
[17] Sashin V A, Bolorizadeh M and Ford M J 2000 *Surf. Sci.* **495** 35
[18] Sashin V A, Canney S A, Ford M J, Bolorizadeh M, Oliver D R and Kheifets A S 2000 *J. Phys.: Condens. Matter* **12** 125
[19] Dirac P A M 1930 *Proc. Camb. Phil. Soc.* **26** 376
[20] Vosko S H, Wilk L and Nusair M 1980 *Can. J. Phys.* **58** 1200
[21] Perdew J P, Burke K and Ernzerhof M 1996 *Phys. Rev. Lett.* **77** 3865
[22] Perdew J P and Ernzerhof M 1996 *J. Chem. Phys.* **105** 9982
Ernzerhof M and Scuseria G E 1999 *J. Chem. Phys.* **110** 5029
[23] Dovesi R, Roetti C, Freyria-Fava C, Apra E, Saunders V R and Harrison N M 1992 *Phil. Trans. R. Soc.* A **341** 203
[24] Wyckoff R 1963 *Crystal Structures* 2nd edn (New York: Interscience)
[25] Soule de Bas B, Dorsett H E and Ford M J 2003 *J. Phys. Chem. Solids* **64** 495
[26] Kheifets A S, Lower J, Nygaard K J, Utteridge S, Vos M, Weigold E and Ritter A L 1994 *Phys. Rev.* B **49** 2113